RASĀYAN *J. Chem.*
Vol. 16 | No. 2 |707-713| April - June | 2023
ISSN: 0974-1496 | e-ISSN: 0976-0083 | CODEN: RJCABP
http://www.rasayanjournal.com
http://www.rasayanjournal.co.in

APPLICATION OF SQUARE WAVE POTENTIAL REGIME TO ELECTRO REDUCTION OF CO_2 IN ETHANOLAMINE INTO ETHYL CARBAMATE BY PALLADIUM ELECTRODE

A.K. Alkhawaldeh[1,✉] and A. Al-Dhuraibi[2]
[1]Department of Medical Allied Sciences, Zarqa University College/ Al-Balqa Applied University, Jordan
[2]Department of Pharmacology and Clinical Pharmacology, Medical Institute, Belgorod National Research University, Russia.
✉Corresponding Author: ahmad.khawaldeh@bau.edu.jo

ABSTRACT
Electrochemical reduction of the CO_2 present in 0.1 M Ethanolamine (EA) aqueous solution at Palladium metal electrodes for the synthesis of ethyl carbamate ($CH_3CH_2OC(O)NH_2$) is investigated. The application square wave potential regime of the carbon dioxide in (EA) to be reduced to an organic product. In addition to identifying optimal conditions for CO_2 electrocatalysis reduction by the square wave potential regime, the potential value was between -1.0 to 0.4 V with 1.4 V amplitude, the time of reaction was 4 hours and the frequency was 100 Hz. We have carried out reactions at various pH levels and different voltages in an alkaline environment to ensure optimal conditions for the production of ethyl carbamate. The palladium catalysts electrode has demonstrated high CO_2 electro-reduction activity to the organic compound. The organic product was analyzed by cyclic voltammetry, NMR, UV spectrometry, FT-IR spectroscopy, TGA, and MS. The results suggest the reduction of CO_2-saturated in 0.1 M ethanolamine to ethyl carbamate, $C_2H_5OCONH_2$. The Faradaic Efficiency and current density of electro-convert CO_2-saturated in ethanolamine to ethyl carbamate are 93% and 71 mA cm^{-2}, respectively.
Keywords: Reduction of CO_2, Potential Regimes, Carbamate, Palladium Electrode, Electroreduction, Square Wave.
RASĀYAN *J. Chem.*, Vol. 16, No.2, 2023

INTRODUCTION

In recent years, global warming has been of serious environmental concern. A large amount of CO_2 is a major reason for this, and if proper action were not taken, it would create serious problems. Significant CO_2 emissions from the burning of fossil fuels contribute to overall temperature rise, adding to overall global warming.[1] Recent research has focused on alternative clean and sustainable energy resources, however, due to population growth, the complete de-coupling of fossil fuels from economic growth is still unfeasible.[2,3] Therefore, the capture and conversion of CO_2 into certain value-added products such as methane, ethylene, carbon monoxide, formaldehyde, formic acid, methanol, and certain derivatives, is a promising alternative solution.[3,4] Various methods have been adapted for the conversion of CO_2 into added-value end products and include photochemical, biological, chemical, photo-electrochemical, and electrochemical technologies.[5] Amongst those methods, the electrochemical reduction of CO_2 is the most feasible and promising route since it is a controllable process with mild operating conditions. The process parameters can be easily adjusted by changing the conditions of electrolysis, such as electrode[6] and electrolytes.[7] Most of the recent research has focused on the development of highly selective products, as product selectivity is crucial in the production of different value-added chemicals via electrochemical reduction of CO_2.[8] However, Faraday efficiency of common electrocatalysis is low, and therefore, the design of efficient and highly selective electrocatalyst is crucial.[9] Depending on the electrochemistry metal catalysts such as platinum, nickel, and Palladium are used, and the reduction of CO_2 can achieve a wide range of products. Electrochemical CO_2, synthesizing various products like HCOOH, methanol, and carbon monoxide, has been applied. These include the presence and handling of fluid products such as methanol (CH_3OH) and HCOOH in comparison to gasses.[10] Different catalytic systems such as Sn, In, or Pb are employed in many electrolytes to manufacture organic produce, using the electrochemical, an ideal catalyst for CO_2 electro reduction requires: (i) having a low overpotential for the activation of the CO_2 molecule;

http://doi.org/10.31788/RJC.2023.1628290

(ii) ability to mediate the transfer of electrons coupled to protons; and (iii) showing selectivity towards a target end product.[11] Applying square wave potential regime in electrochemistry reduction of CO_2 used to reduce the applied overpotential and increase the efficiency of the catalysts.[12] Controlling the square wave potential in the electrochemical reduction of CO_2, the negative impact of over potential is reduced, subsequently increasing the catalyst efficiency. In addition, to catalyst choice, the selection of a suitable electrolyte that stabilizes the system is critical.[13] The electrolyte acts as a transfer median of charge between the co-catalyst and the electrodes during the electrochemical reaction, the system is stabilized through the proper selection and use of electrolyte. The conversion of CO_2 in both non-aqueous and aqueous electrolytes is currently feasible. As aquatic electrolytes, the water-based solutions K_2SO_4, $KHCO_3$, K_2CO_3, Na_2SO_4, Na_2CO_3, and $NaHCO_3$.[14] In addition, in electrical decreasing CO_2, the CO_2 solutions also play a significant role in the electrolyte.[15] The improved solubility of CO_2 improves the process of CO_2 reduction, which ultimately Increases Faradaic efficiencies of converting CO_2.[16] The Faradaic efficiencies rely on various reactors, as well as, electrolytes and electrodes. For optimum Faradaic efficiencies and effective CO_2 conversion, the construction of a proper reactor is crucial.[17] For the optimum operating condition for the reduction of CO_2, they have utilized several catalyst materials like Sn, Ru, and Pd at various electrolytic pH.[18] In this study, the electroreduction of CO_2-saturated in 0.1M ethanolamine by using a Pd electrode in a square wave potential regime to the useful organic product. At atmospheric pressure and room temperature, experiments have been carried out.

EXPERIMENTAL

Material and Methods

All square wave potential regimes and cyclic voltammetric experiments were carried out using potentiostat 273A (Princeton Applied Research), equipped with Echem® software, allowing for precise potential control. Using a function generator (Bk Precision, 4003A), a square wave with the selected frequency and amplitude was produced. An electrochemical cell containing ethanolamine solution and CO_2 saturated was sealed tightly with a rubber stopper. The cell contained three working electrodes (Polycrystalline Palladium foil 1-cm^2 in diameter, 99.95% pure, Palladium was purchased from Sigma Aldrich), the auxiliary electrode (platinum gauze plate 3-cm^2 platinum, Aldrich, 99.99%), and the Ag/AgCl/ [Cl^-] reference electrode. Samples (10 mg) were held in open platinum pans (110 µL). The International Company for Medical and Industrial Gases supplied 99.999% pure G5 grade nitrogen gas and CO_2 (Jordan). All reagents were analytical (A.R) grade certified. Ethanolamine ($NH_2CH_2CH_2OH$, 97%, Fluka, Germany) and Sulfuric acid (97%, Merck, Germany) were dissolved in Milli-Q water (Millipore, Merck). IR scanning spectra for the isolated matter from the treated solution embedded in the KBr matrix were used (Thermo Nicolet Nexus-670) FTIR spectrophotometer for the accessible wave number range between 4000 and 400 cm^{-1}. On a Brucker (Avance III 500 MHz), an NMR spectrum spectrometer (^{13}C, ^1H-NMR, and DEPT 135) was obtained. The UV-VIS spectra were recorded by Varian Cary 100 UV-VIS spectrophotometer. Applied Biosystems/MDS-SCIEX-Api-3000 (LC/MS/MS), rate 10.0 µl/min. Thermogravimetric analysis, with a heating rate ranging from the Netzsch thermal Analyzer (model STA 409 PC/PC) was used to measure temperatures between 50 - 1000 ºC at a rate of 5 ºC/min. Thermal measurements use for studying the physical and chemical properties of the solid organic sample. To determine the physicochemical properties of the organic solid sample, the TGA was carried out at temperatures ranging between 10-800 C°, with a heating rate of 10 C°/minute. The TGA (STA 409 PC/PC) used nitrogen purge gas under constant flow.

General Procedure

All glassware used in experiments of the square wave and cyclic voltammograms was cleaned by dipping it in a chromic acid solution and rinsing it with Milli-Q water. The work electrode Palladium was cleaned by negative/positive scan between -0.2 to 1.2 V in the cell. The Ethanolamine 0.1M solution was saturated with CO_2 by continuously flowing and bubbling for 15 minutes at room temperature. The pH of the ethanolamine solution was 12, and after bubbling with CO_2 gas for 15 minutes dropped to 8.5. Using a square wave to electro-reduction carbon dioxide in a cell for 4h at a Palladium electrode, the potential was between -1.0 mV to 0.4 mV, the current was 1µA and the frequency was 100Hz.

Detection Method

The cyclic voltammograms (CV) of Palladium electrode in 0.5 M sulfuric acid, purging solution by nitrogen gas to remove oxygen-free on the cell, the cyclic voltammogram was used to detect organic species of the solution and for the purpose of detecting any modification to the solution's chemistry. The cyclic voltammogram and square wave potential regime experiments were performed at ambient conditions. The organic product generated after the application of a square wave potential in CO_2-saturated 1.0 M ethanolamine was analyzed by NMR, IR, TGA, MS, and cyclic voltammogram.

RESULTS AND DISCUSSION

Figure-1 shows cyclic voltammograms obtained in 0.5M H_2SO_4 with the scan rate of 100 mV/s over the potential range from −0.20 to 1.20 V, for pure platinum and treated platinum electrode (solid and dashed line, respectively). The typical voltammetric pattern of the Pt electrode was observed. Cyclic voltammograms of the treated Pt electrode display a peak, which was assigned to the oxidation of organic compounds in solution at 0.3V after electrochemistry reduction of CO_2. Figure-1 shows a representative CV of Pt electrode with a 5 ml solution after application square wave potential in CO_2 saturated in 0.1M ethanolamine, the peak centered in dashed line CV at 0.3V, increase in the oxygen adsorption region and decreases in the hydrogen adsorption/desorption were indicative of the presence of organic product in the cell. This finding offers unambiguous proof that these peaks were organic species present in bulk solution.[19] As a result, the application of the square wave to the Pd electrode in CO_2-saturated 0.1M ethanolamine solution revealed the first event in the Pt electrode's CV, demonstrating the creation of a new substance.

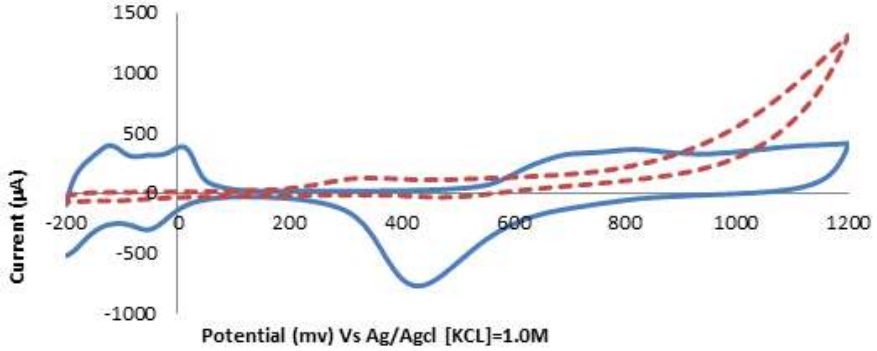

Fig.-1: CV of Pt Electrode of Ethanolamine Without CO_2 (——) and (…….) 0.5M H_2SO_4 with 5ml Treated CO_2

Figure-2 displays the UV-VIS molecular spectrum of the organic species after applying a square wave at 200-400 nm. The ultraviolet spectrum gives information about finding an organic product by application square wave to reduce CO_2 in a 0.1M ethanolamine solution. The presence of two functional groups in the chemical structure of the sample was observed. This result depends on two adsorption peaks at different wavelengths (at 233 and 332 nm) in the ultraviolet region. It is well-known that the organic product after applying a square wave of CO_2 saturated in 0.1M ethanolamine solution at the Palladium electrode exhibits two absorption bands due to the $\pi \rightarrow \pi^*$ transitions from (HOMO) to (LUMO). UV-VIS absorption spectrometry is evidence for converting CO_2 to organic species upon using a potential regime of a square wave to a Pd electrode.

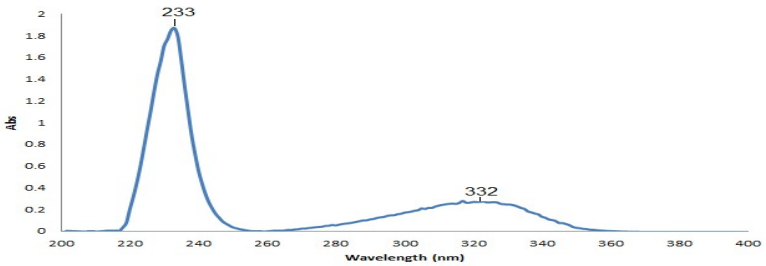

Fig.-2: UV-Vis Spectrum Absorption of the Organic Product for CO_2 Saturated in 0.1M Ethanolamine

Figure-3 shows the mass spectrum upon analysis by MS to determine molecular weight and fragmentation of the electroreduction products of CO_2 at the Pd electrode upon using a potential regime of a square wave

in 0.1M ethanolamine solution. The major ion observed in Fig.-3 spectrum was at 89.0 m/z for an unfragmented molecule of the specimen. The mass fragments of the organic product were broad: 89.0 m/z (small peak, $C_3H_7NO_2$), 73.7 m/z (small peak, $C_3H_5O_2$), 59.2 m/z (large peak, $C_2H_3O_2$), 44.1 m/z (medium peak, CO_2). The other peaks shown in the figure may come from electrolyte impurities. The major ion observed in the MS spectrum was at m/z 89.0 for the organic product by application square wave regime was ethyl carbamate.

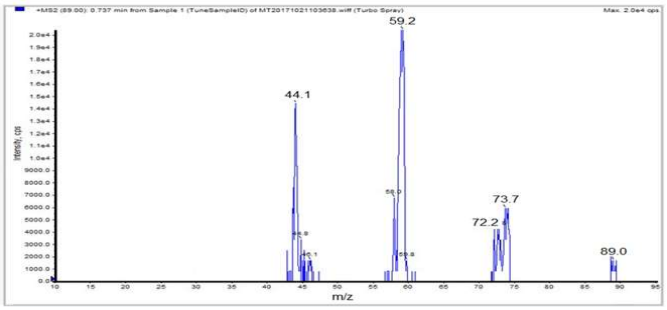

Fig.-3: The Mass Spectra of Product ions and Fragmentation Pattern for the Produced Compound for CO_2 Saturated 0.1M Ethanolamine

Fourier Transform Infra-Red (FTIR) spectroscopy was used to identify the functional groups present in the organic compound product after the application of square wave potential of CO_2 in a 0.1M ethanolamine solution for 4 hours using a Palladium electrode. Figure-4 shows the IR spectrum of the organic sample collected after drying the solution using the KBr pellet technique. The assigned bands are presented in Table-1.

Table-1: The Vibrational Frequencies of Various Functional Groups of Organic Products and the Assignments Corresponding to the Peaks

Frequencies	Functional groups	Frequencies	Functional groups
3346.28 cm^{-1}	N–H stretching	1620.65 cm^{-1}	carbonyl (C=O) vibration
3120.55 cm^{-1}	symmetric vibrations NH_2	1477.99 cm^{-1}	carboxylate (O-C=O)
2976.97 and 2901.62 cm^{-1}	CH_2 and CH_3	1344.60 cm^{-1}	C-O
2537.18 cm^{-1}	C=O stretching	830.99 cm^{-1}	C-N

The infrared data supports the conclusion that the reduction product contains two functional groups. Since the compound contains conjugated C=O bond NH_2 as indicated by UV-VIS data, as indicated by mass spectrometric results. Based on the FTIR spectrum in Fig.-4 and Table-1, it is obvious that the organic compound produced using a square wave potential regime at CO_2-saturated in a 0.1M ethanolamine solution is consistent with our comparison of IR spectra for ethyl carbamate.

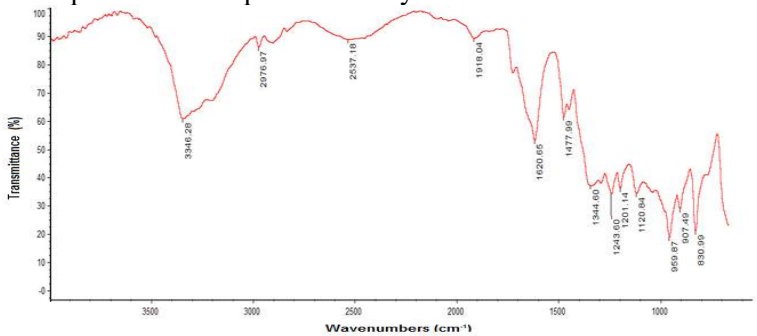

Fig.-4: IR- Spectrum for the Produced Organic Compound from the CO_2 Saturated 0.1 M Ethanolamine

The NMR spectroscopy (^1H, ^{13}C-NMR, and DEPT 135), presented in Fig.-5, shows chemical shifts of the organic product by application of a square wave potential regime to a palladium electrode in CO_2-saturated in 0.1M ethanolamine. In the ^1H NMR spectrum (Fig.-5A), the hydrogen peaks are observed at 1.21 triple peak, 4.01 quartzite peak, and 4.70 ppm signal peak. Similarly, the proton (in ethyl carbamate) chemical shifts are in the range of 1-5 ppm. The chemical shifts obtained for an H1 atom of the CH_3 group are quite

low, H_2 and H_3 are higher due to proton bonding on the oxygen site, whereas the localization of proton was similar for ethyl carbamate. The ^{13}C-NMR (Fig.-5B) gives three signals in overlapped areas of the spectrum with chemical shift values at 11.49, 48.85, and 205.71 ppm. The C1 (CH_3- group) signal was observed at 11.49 and C2 (-CH_2-O- group) signal was observed at 48.85 ppm. The chemical shift of C3 (206.71 ppm) was recognized by (O-C=O carboxylic groups). The C3 atom was deshielded due to the presence of electronegative oxygen in the carboxylic group. Besides, the chemical shifts value in DEPT 135 (Fig.-5C) shows the different types of carbon in the spectrum of the organic compound (which indicates including of CH_3 at 11.22 ppm and CH_2 at 4859 ppm groups). In our present investigation, the experimental chemical shift value of the organic compound indicates ethyl carbamate.

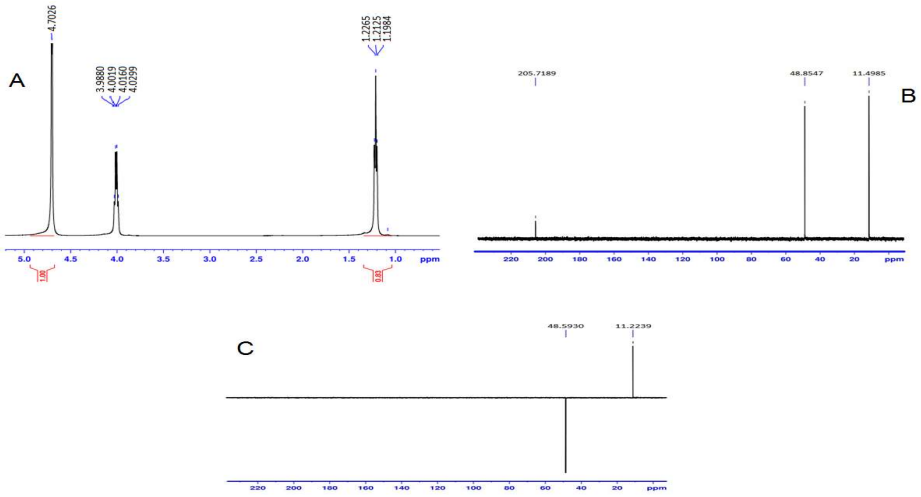

Fig.-5: NMR Spectra of (A) ^{1}H- NMR; (B) ^{13}C-NMR and (C) DEPT 135 for the Produced Organic Compound from the CO_2 Saturated 0.1M Ethanolamine

Thermal measurements were conducted in studying the physical and chemical properties of the solid organic sample, and are shown in Fig.-6. The organic compound was produced by the electroreduction of CO_2 in an ethanolamine solution. The TGA trace of the solid sample also exhibited two thermal events before being sample consumed. The measurements of loss in mass with time were recorded at two stages: (i) stage one performed between 100 to 200 °C with mass loss of 28.41% (which corresponds to the decomposition of CO); and (ii) stage two recorded between 220 to 350 °C with mass loss of 47.75% (which corresponds to decomposition of ethanol $CH_3{-}CH_2{-}OH$). The residual mass per unit time at temperature 779.3 °C was 19.13% and is due to the presence of supporting electrolyte residues in the sample. TGA confirmed organic product structure was ethyl carbamate.[20]

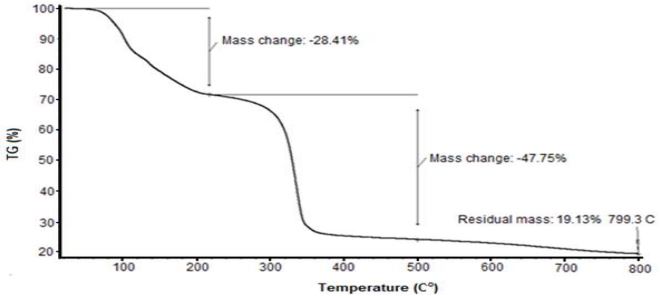

Fig.-6: TGA Analysis of Organic Compound, Produced From the CO_2 Saturated 0.1M Ethanolamine

The reaction between CO_2 and ethanolamine depends on the role of the surfactant for the palladium electrode. The structure of the palladium metal has an electrocatalytic active site that plays an essential role in the electro-reduction of CO_2. During the application of the square wave potential regime carbon dioxide and ethanolamine are coupled to the active surface. The results show that carbamate formation in accordance with the zwitterion mechanism began in the absorption phase of Ethanolamine (EA). Mechanistic details of the reaction have been studied. Initially, a CO_2 molecule reacts with ethanolamine

to form the carbamic acid ($EACOO^-$) major species, and CO_3^-/CO_3^{2-} were minor species, followed by the hydration of CO_2 to form HCO_3^-/CO_3^{2-}, and finally HCO_3^- reacts with carbamic acid to form carbamate[20], as displayed below in eq.-1.

$$CO_2 + EA \rightleftharpoons EACOO^- + HCO_3^- \rightleftharpoons EACOOH. \quad (1)$$

An essential factor in figuring out the rate at which CO_2 is reduced electrochemically is the current density. The current of electrolysis is influenced by the use of a constant cell voltage. Therefore, as shown in eq.-2, current density (j) is defined as the relationship between current I and the geometric work electrode surface (A).

$$j = \frac{i}{A} \quad (2)$$

Faradaic performance is another major guide for the assessment of product mixing and CO_2 reduction electrochemical selectivity. The charge ratio for a total manufactured product (αNF) is indicated, while α is the number of transfers of electrons; The desired item is N. mole; and The faraday constant is F of 96 485, C mol^{-1}) is shown by eq.-3 to the total electrical charge incurred (Q).[21]

$$E = \frac{\alpha NF}{Q} \quad (3)$$

Table-2: A list of Different Materials for CO_2 Reduction Electrochemically. Details Included Catalysts, Current Density, Faradaic Efficiency, and Electrolytes

Catalyst	Current Density	Faradaic Efficacy	Electrolyte	Ref
MoS_2	65 mA cm^{-2}	98%	water	22
TiO_2	68 mA cm^{-2}	85%	Potassium bicarbonate	23
Nickel	1.45 mA cm^{-2}	90%	Potassium bicarbonate	24
Graphene	10.2 mA cm^{-2}	92%	Potassium bicarbonate	25
Pd	71 mA cm^{-2}	93%	Ethanolamine	My work

CONCLUSION

Convert CO_2 to solid organic compound (ethyl carbamate) in an electroanalytical cell by square wave potential regime between -1.0 to 0.4 V with 1.4 V amplitude, frequency 100 Hz, and time of reaction was 4h. The product of the application square wave potential to a palladium electrode in 0.1M ethanolamine saturated with CO_2 was Ethyl carbamate. It was proved by NMR, IR, UV, TGA, MS, and cyclic voltammetry; Such methods have been used have used these techniques to determine the structure and fragmentation of organic compound products after the reduction of carbon dioxide of the sample collected after the applied square wave.

ACKNOWLEDGMENTS

Authors are thankful to the authorities of their institutions for providing their cooperation and support.

CONFLICT OF INTERESTS

The authors declare that there is no conflict of interest.

AUTHOR CONTRIBUTIONS

All the authors contributed significantly to this manuscript, participated in reviewing/editing and approved the final draft for publication. The research profile of the authors can be verified from their ORCID ids, given below:

A. K. Alkhawaldeh http://orcid.org/0000-0003-4348-6613
A. Al-Dhuraibi https://orcid.org/0000-0002-9044-243X

REFERENCES

1. L. Xu, Y. Xiu, F. Liu, Y. Liang, and S. Wang, *Molecules*, **25(16)**, 3653(2020), https://doi.org/10.3390/molecules25163653
2. A. Duwe, N. Tippkötter, and R. Ulber, *Advances in Biochemical Engineering/Biotechnology*, ABE,volume 166, pp.177–215(2017), https://doi.org/10.1007/10_2016_72
3. A. Goeppert, M. Czaun, J.-P. Jones, G.K. Surya Prakash, an G.A. Olah, *Chemical Society Reviews,* **43**, 7995(2014), https://doi.org/10.1039/c4cs00122b
4. H.-R."M. Jhong, S. Ma, and P.J.A. Kenis, *Current Opinion in Chemical Engineering*, **2(2)**, 191(2013), https://doi.org/10.1016/j.coche.2013.03.005
5. K. Malik, B.M. Rajbongshi, and A. Verma, *Journal of CO_2 Utilization*, **33**, 311(2019), https://doi.org/10.1016/j.jcou.2019.06.020
6. U. Fegade, and G. Jethave, *Technology*, **2**, 91(2019), https://doi.org/10.1007/978-3-030-28638-5_4
7. A. Pandiarajan, R. Sekar, K. Pavithra, M. Gomathi, S.M. Senthil Kumar, and M. Anbu Kulandainathan, *Journal of Applied Electrochemistry,* **53(5),** 1033(2022), https://doi.org/10.1007/s10800-022-01815-6
8. V.S. Yadav, and M.K. *Purkait, New Journal of Chemistry*. **39(9)**, 7348(2015), https://doi.org/10.1039/c5nj01182e
9. H.A. Hansen, J.B. Varley, A.A. Peterson, and J.K. Nørskov, *The Journal of Physical Chemistry Letters*. **4(3)**, 388(2013), https://doi.org/10.1021/jz3021155
10. A. Al Khawaldah, *Journal of Oleo Science*, **72(3),** 347(2023) https://doi.org/10.5650/jos.ess22376
11. K. Park, G.H. Gunasekar, and S. Yoon, *CO_2 Hydrogenation Catalysis,* pp.149-177(2021), https://doi.org/10.1002/9783527824113.ch6
12. B.S. Yeo, *ECS Meeting Abstracts,* **MA2019-01(33)**, 1709(2019), https://doi.org/10.1149/ma2019-01/33/1709
13. H. Xiang, S. Rasul, K. Scott, J. Portoles, P. Cumpson, and E.H. Yu, *Journal of CO_2 Utilization,* **30**, 214(2019), https://doi.org/10.1016/j.jcou.2019.02.007
14. X. Ye, and Y. Lu, *Chemical Engineering Science*. **116**, 657(2014), https://doi.org/10.1016/j.ces.2014.05.050
15. V.S. Yadav, and M.K. Purkait, *RSC Advances*, **5(50),** 40414(2015), https://doi.org/10.1039/c5ra05899f
16. O. Scialdone, A. Galia, G.L. Nero, F. Proietto, S. Sabatino, and B. Schiavo, *Electrochimica Acta,* **199,** 332(2016), https://doi.org/10.1016/j.electacta.2016.02.079
17. C. Zhao, and J. Wang, *Chemical Engineering Journal,* **293**, 161(2016), https://doi.org/10.1016/j.cej.2016.02.084
18. M. Sassenburg, R. de Rooij, N.T. Nesbitt, R. Kas, S. Chandrashekar, and N.J. Firet, *ACS Applied Energy Materials,* **5(5)**, 5983(2022), https://doi.org/10.1021/acsaem.2c00160
19. Y. Wu, and W. Liu, *Fuel*, **285**, 119165(2021), https://doi.org/10.1016/j.fuel.2020.119165
20. Z. Sun, T. Ma, H. Tao, Q. Fan, and B. Han, *Chem*, **3(4)**, 560(2017), https://doi.org/10.1016/j.chempr.2017.09.009
21. M. Asadi, B. Kumar, A. Behranginia, B.A. Rosen, A. Baskin, and N. Repnin, *Nature Communications*. **5(1),** (2014), https://doi.org/10.1038/ncomms5470
22. P. Su, K. Iwase, S. Nakanishi, K. Hashimoto, and K. Kamiya, *Small*, **12(44)**, 6083(2016), https://doi.org/10.1002/smll.201602158
23. W. Bi, X. Li, R. You, M. Chen, R. Yuan, and W. Huang, *Advanced Materials,* **30(18)**, 1706617(2018), https://doi.org/10.1002/adma.201706617
24. S. Dongare, N. Singh, and H. Bhunia, *Journal of CO_2 Utilization,* **44**, 101382(2021), https://doi.org/10.1016/j.jcou.2020.101382
25. H. Li, N. Xiao, M. Hao, X. Song, Y. Wang, and Y. Ji, *Chemical Engineering Journal*, **351**, 613(2018), https://doi.org/10.1016/j.cej.2018.06.077

[RJC- 8290/2022]